

Membrane Mirror Light Modulator Technology

C. Warde¹, J. McCann², V. Shrauger, H. Jeong, A. Ersen, X-Y Wang and J. Hubbard

Optron Systems, Inc., 3 Preston Court, Bedford, MA 01730, USA

We have incorporated membrane mirror technology over a discrete array of pixel wells to create both high-efficiency optical shutters and spatial light modulators (SLM). A continuous metalized-membrane mirror with greater than 98 reflectivity minimizes optical insertion loss. This mirror is electrostatically deformed into the wells with either a common electrode (shutter) or pixelated electrodes (SLM). By using a spatial filter, analog intensity optical modulation is realized. Both 1-D (linear) and 2-D grating pixel patterns have been investigated. With the appropriate pixel dimensions, both coherent monochromatic and broadband incoherent light within the 0.25 to 10.6 micron range can be modulated with contrast ratios up to 1000:1. Small well sizes (approximately 10-micron diameter) allow for modulation speeds up to 1 MHz. The theoretical foundations for the well layout, the membrane mirror deformation and its diffraction properties, and the design trade-offs are detailed. We have applied our membrane mirror technology to CMOS VLSI circuits creating a high-speed, high-efficiency spatial light modulator capable of 80x64 resolution and scalable to HDTV standards. The membrane mirror SLM provides either amplitude or phase modulation- in the phase modulation mode, at least two waves of stroke per discrete well are possible.

Keywords: shutter, membrane mirror, light valve, spatial light modulator

1. Introduction

Membrane mirror light modulation (MLM) technology has been in existence for over thirty years [1]. This technology incorporates a deformable membrane mirror as the light-modulating element over an array of addressing electrodes. These devices exhibit very fast response times (microsecond rise times), can be read out with high optical efficiency, and may contain large numbers of resolution elements. The advantages of MLM devices are that they will perform amplitude or phase modulation of light over a wide wavelength range, the modulation is relatively polarization independent, and they can tolerate relatively high optical powers without damage. Thus, membrane mirror light modulators are attractive for applications such as adaptive optics, projection display, and optical signal processing [2-4].

Several means of addressing a two-dimensional deformable membrane have been demonstrated, including electron beam addressing, [5] optical addressing, [3,6-8] and electrical addressing via integrated circuits [1,9,10]. Other addressing schemes include discrete electrodes, row-column electrode patterns, thin-film transistor arrays, matrix-addressed electrodes, electron guns [11], photoconductors, photodiodes and phototransistors.

We have built membrane mirror light shutters with a single electrode common to all the pixels, and with a small number of discrete hard-wired electrodes addressing the entire device. We have also built high-resolution spatial light modulators that are addressed with electron guns [11], photoconductors and VLSI chips. Some of this work is summarized in this paper.

2. Device Description and Principles of Operation

As shown in Fig.1, the MMLS consists of a substrate that supports a 2-D array of wells that are etched into an

¹ Massachusetts Institute of Technology, Cambridge, MA 02139, USA.

² M. J. C. Corporation, 150 G. St., Keene, NH 03431, USA.

insulating layer atop the substrate. A thin metal-coated membrane-mirror bonded to the insulating layer covers the wells. A second electrode located at the base of the wells allows voltages to be applied across the wells to electrostatically deform the membrane mirror into the wells. Devices employing both one-dimensional (grating lines) and two-dimensional patterns (rectangular and hexagonal grids) of pixel wells have been fabricated. This assembly is sealed in an evacuated housing that is fitted with a readout window. The electronic control unit is a high-voltage, high-bandwidth amplifier that can be fed by a signal/pulse generator. It can also provide a dc offset that is necessary for certain modes of operation of the MMLS. The spatial filter is either a circular aperture or a circular opaque disc positioned at the center of the focal plane of the Fourier lens.

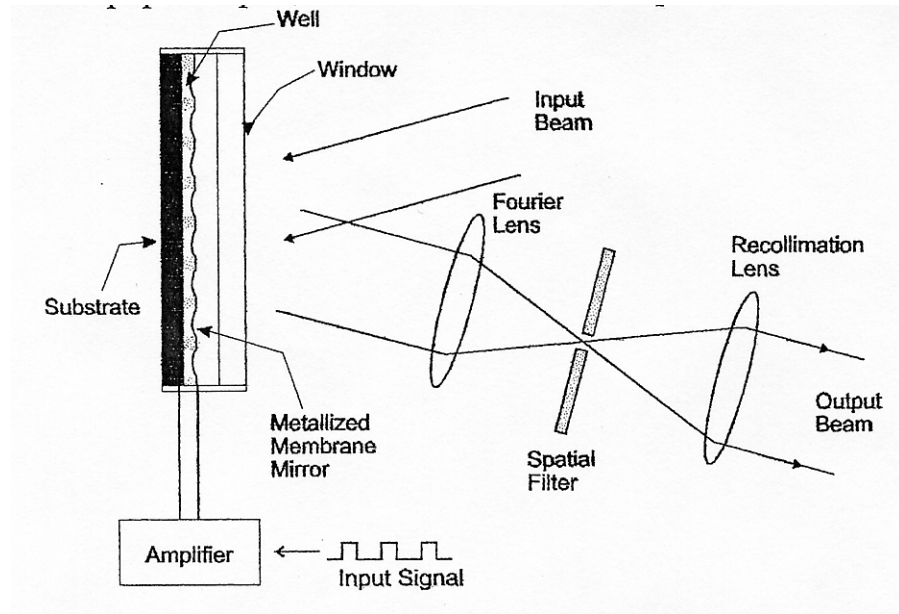


Figure 1: Architecture of the membrane-mirror light shutter system with zero-order pass spatial filtering

2.1. Zero-Order-Pass and Zero-Order Stop Operations

In zero-order-pass operation, the Fourier-plane spatial filter is a circular aperture. The light to be modulated or chopped (incoherent or coherent, polarized or unpolarized) is nominally collimated before it reaches the MMLS (see Figure 1). Typically up to 10° full cone angle of divergence can be tolerated. When there is no voltage across the wells, the membrane mirror is flat and the light reflecting off the shutter surface maintains its collimation. Thus, the Fourier transform lens focuses this light to a single zero-order spot which passes through the spatial filtering aperture and is recollimated by the second lens as shown. This corresponds to the on state of the shutter. In this case, essentially all the light reaching the modulator is recovered as on-state radiance. If a small-diameter laser beam is used (e.g., 2-5 mm) no lenses are necessary. Generally, in this case, the zero order light is well separated from the higher orders and is easily filtered out.

When a voltage waveform is applied to the electrodes, the resulting electrostatic forces deform the membrane mirror into the underlying wells, and the membrane mirror becomes a 2-D diffraction grating. As the voltage across the wells increases, the deformation of the membrane-mirror increases, and more and more light is scattered out of the zero order into higher orders leading to lower and lower zero-order output intensity. Thus, gray-scale intensity modulation is achieved. At some specific applied voltage, V_a , the zero-order light is extinguished and the off-state is achieved. The modulator may be driven with square waves or pulses for binary on/off operation, or with sine waves, triangular waves, or any arbitrary waveform.

In zero-order-stop operation, the Fourier-plane spatial filter is an opaque disc positioned at the center of the Fourier plane. In this mode, the output light is off when there is no voltage across the wells. This is because the mirror surface is undeformed and all of the light reflected from the shutter is blocked by the zero-order stop. When voltage is applied across the wells, the membrane mirror deforms into the wells and a voltage-dependent

portion of the light then diffracts around the stop into higher orders. This light is collected by the recollimation lens to form the output signal. At the extinction voltage, V_a , all of the power is in the non-zero order light and the fully on state is achieved. The contrast ratio in this mode can be extremely high especially at infrared wavelengths.

3. Device Modeling and Experimental Results

3.1. Operating Voltage

Under the influence of the electrostatic forces, the membrane mirror deforms into the wells with a parabolic profile. The behavior of a circularly bounded, parabolically deflecting pixel is such that the deflection at the center of the pixel (representing maximum deflection) may be modeled by [6]

$$d = \frac{\epsilon_0 a^2 V^2}{32 T s^2}$$

where a is the well diameter, s is the well depth, T is the membrane tension, V is the voltage across the well, and ϵ_0 is the permittivity of free space. Thus, it is seen that the operating voltage scales as the ratio of well depth to well diameter, and as the square root of the membrane tension. Typical extinction voltages for visible light can range from as low as 30 V for 100- μ m wells to above 200 V for 10-nm wells. The extinction voltage also increases with increasing wavelength, as expected.

3.2. Light Modulation Characteristics: Diffraction Theory

The light modulation of the MMLS can be studied by considering the device as a diffractive reflective surface with a variable phase profile. Thus, Fourier analysis can determine the spatial distribution of the readout light [12-14]. Although the working devices are two-dimensional, the fundamental operation can be understood by considering the one-dimensional case of a reflective phase grating with uniform reflectance. The following analysis assumes illumination by an infinite extent monochromatic plane wave at normal incidence. This does not cause any loss of generality, as the diffraction pattern under real illumination, from a source such as a laser or a finite aperture, will change only in the shape of the individual diffracted spots. These will assume the shape of the Fourier transform of the aperture.

The deformation of the membrane is assumed to take a periodic, parabolic deflection profile. This is based on electrostatic deflection theory for thin membranes and also experimental observation. A cross section of the membrane mirror in deflection is shown in Figure 2. In this figure, one period of the structure is illustrated as T with the well width given as a and the maximum deformation depth given as d .

The depth function over one period is expressed by the following:

$$z(x) = \begin{cases} d(1 - \frac{4x^2}{a^2}) & -\frac{a}{2} \leq x \leq \frac{a}{2} \\ 0 & \frac{a}{2} \leq |x| \leq \frac{T}{2} \end{cases}$$

The reflectance function is expressed as:

$$r(x) = r_0 e^{-i2kz(x)} \quad -\frac{T}{2} \leq x \leq \frac{T}{2} \quad \text{and} \quad k = \frac{2\pi}{\lambda}$$

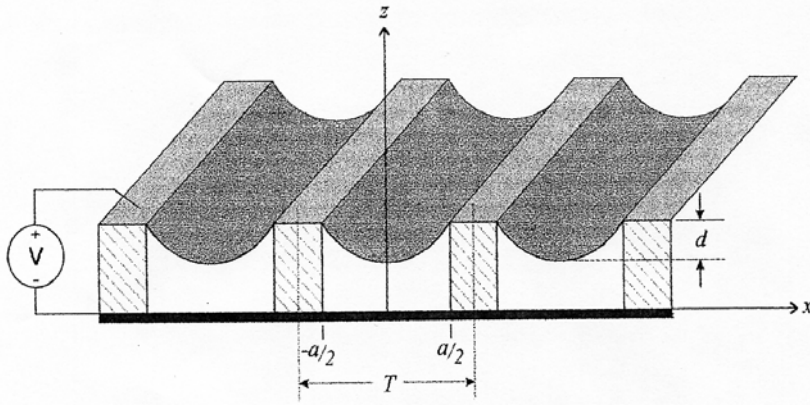


Figure 2: View of general one-dimensional parabolic membrane mirror grating

Since the reflectance function is periodic, the diffracted amplitude can be expressed as a Fourier Series with the coefficients given by:

$$u_m = \frac{1}{T} \int_{-\frac{T}{2}}^{\frac{T}{2}} r(x) e^{-i\left(\frac{2\pi m}{T}\right)x} dx \quad (1)$$

with $-\infty \leq m \leq \infty$, where m is an integer.

For many applications it is the zero order intensity that is of the most interest. This is important in configurations where the higher orders are typically blocked and the zero order is allowed to pass through such as in marking and printing systems. These systems require the device to switch the power in a laser beam continuously from full on to full off with maximum contrast, in this arrangement the zero order beam is typically used to mark a pixel and the higher orders are blocked. A further requirement is that the zero order energy be continuously variable to effect gray scale imaging.

For the zero order term, $m = 0$, and with $r_0 = 1$, the amplitude coefficient is:

$$u_0 = \frac{1}{T} \int_{-\frac{T}{2}}^{\frac{T}{2}} r(x) dx = \left(1 - \frac{a}{T}\right) + \frac{e^{-2ikd}}{T} \int_{-\frac{a}{2}}^{\frac{a}{2}} e^{i8kd\frac{x^2}{a^2}} dx \quad (2)$$

The zero-order intensity is given by the relation $I_0 \propto |u_0|^2$ and the result shown in Figure 3 is obtained by numerical integration of the above with: $\lambda = 0.6328 \mu\text{m}$, $a = 70 \mu\text{m}$, $T = 100 \mu\text{m}$, and $0 < d < 1.5 \mu\text{m}$.

It is also instructive to compute the diffracted intensity for the higher orders as a function of membrane mirror deformation. Higher-order-pass (zero-order block) operation is employed in certain imaging applications and two-port light switching applications. To determine the intensity distribution in the higher orders, we allow for $m \neq 0$ in equation 1, which results with the following:

$$u_m = \frac{1}{T} \int_{-\frac{T}{2}}^{\frac{T}{2}} r(x) e^{-i\left(\frac{2\pi m}{T}\right)x} dx = \frac{1}{T} \int_{-\frac{T}{2}}^{\frac{T}{2}} e^{-i2kd\left(1 - \frac{4x^2}{a^2}\right)} e^{-i\left(\frac{2\pi m}{T}\right)x} dx$$

$$\text{with } \phi = \frac{2\pi m}{T} \text{ and } \alpha = \frac{8kd}{a^2} = \frac{16\pi d}{\lambda a^2};$$

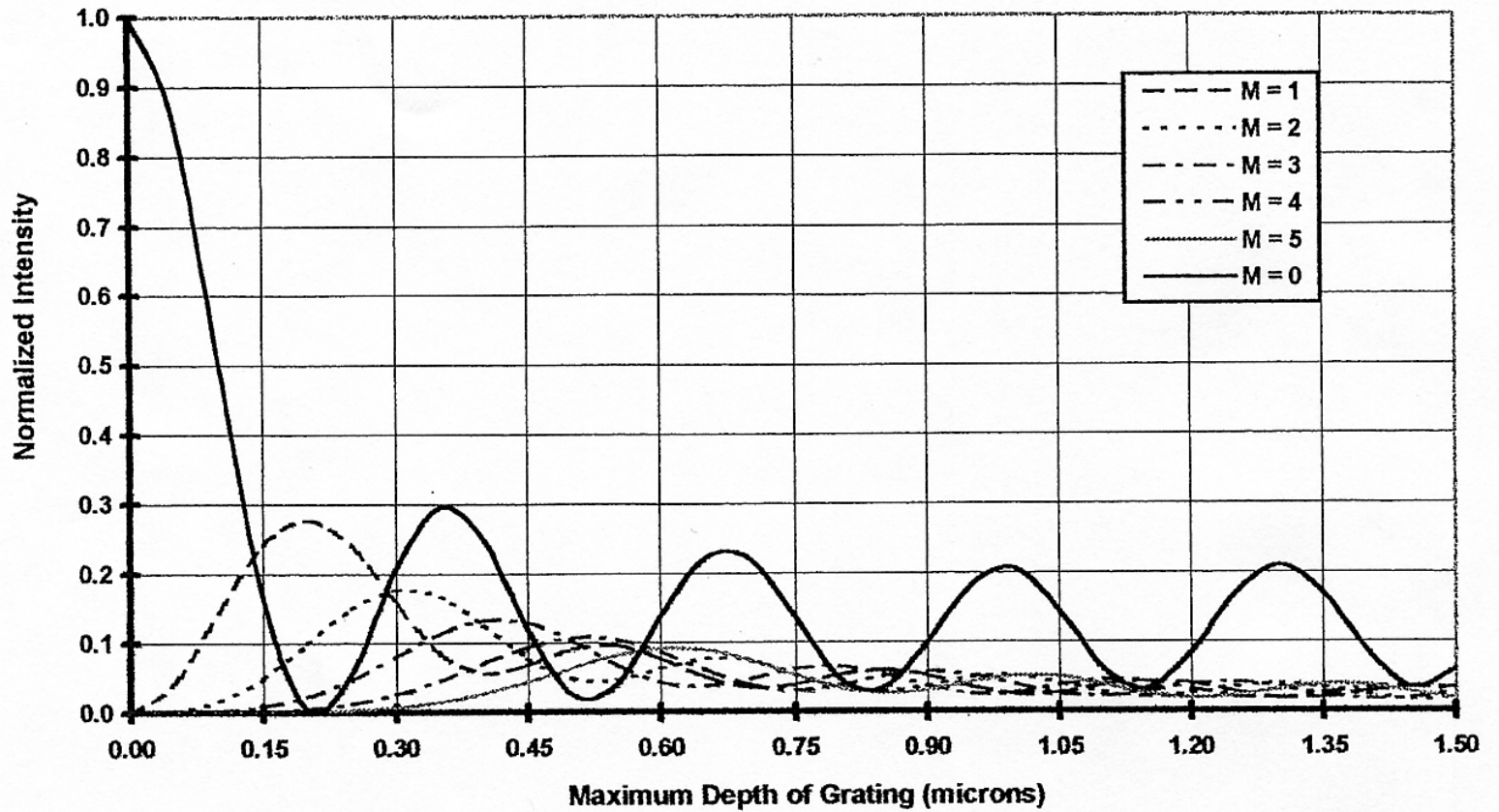


Figure 3: Intensity distribution of the various orders for a one-dimensional (linear grating) membrane modulator as a function of membrane deformation.

$$u_m = \frac{1}{T} \int_{-\frac{a}{2}}^{\frac{a}{2}} e^{-i\phi x} dx + \frac{1}{T} \int_{\frac{a}{2}}^{\frac{T}{2}} e^{-i\phi x} dx + \frac{1}{T} \int_{\frac{a}{2}}^{\frac{a}{2}} e^{-i2kd} e^{i\alpha x^2} e^{-i\phi x} dx$$

which yields

$$u_m = -\left(\frac{1}{\pi m}\right) \left\{ \sin\left(\frac{\pi m a}{T}\right) \right\} + \frac{e^{-2kd}}{T} \int_{\frac{a}{2}}^{\frac{a}{2}} e^{i\alpha x^2} e^{-i\phi x} dx \quad (3)$$

A check on equation 3 is found when $d = 0$. That is, when the membrane is undeflected, all the light is reflected into the zero order and none diffracted, in this case, $-i2kd = 0$, and with $a = 0$ the following is obtained.

$$u_m = -\left(\frac{1}{\pi m}\right) \left\{ \sin\left(\frac{\pi m a}{T}\right) \right\} + \frac{1}{T} \left\{ \int_{\frac{a}{2}}^{\frac{a}{2}} \cos\left(\frac{2\pi m x}{T}\right) dx \right\}$$

$$u_m = -\left(\frac{1}{\pi m}\right) \left\{ \sin\left(\frac{\pi m a}{T}\right) \right\} + \left(\frac{1}{\pi m}\right) \left\{ \sin\left(\frac{\pi m a}{T}\right) \right\} = 0 \quad \text{as required}$$

The intensity is calculated as I_n , a $[U_m \cdot U_m^*]$ and numerical evaluation yields the family of curves shown in Figure 3 for higher order diffraction out to 5th order. One can clearly see that each order has a different membrane depth where its peak intensity is a maximum.

Figure 4 is the measured zero-order-pass output intensity characteristic of an MMLS system with 1-D pixel wells on a 20 μm pitch, read out at 633 nm. Note that V^{\wedge} is approximately 136 V for this device. The measured contrast ratio exceeds 1000:1. Note that the light modulation characteristic is a non-linear function of voltage. Linear analog response (AI a AV) which is required for some analog operations, can be achieved by using look-up table techniques, or by amplifying the drive electrical signal with voltage-dependent gain.

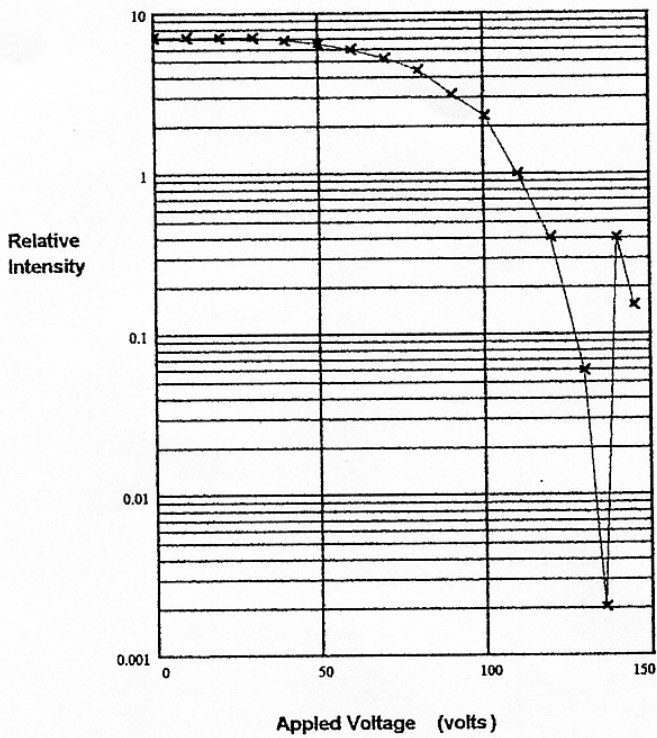


Figure 4: Static zero-order-pass output intensity of an MMLS with 1-D pixel wells on a 20 μm pitch for 633 nm laser light.

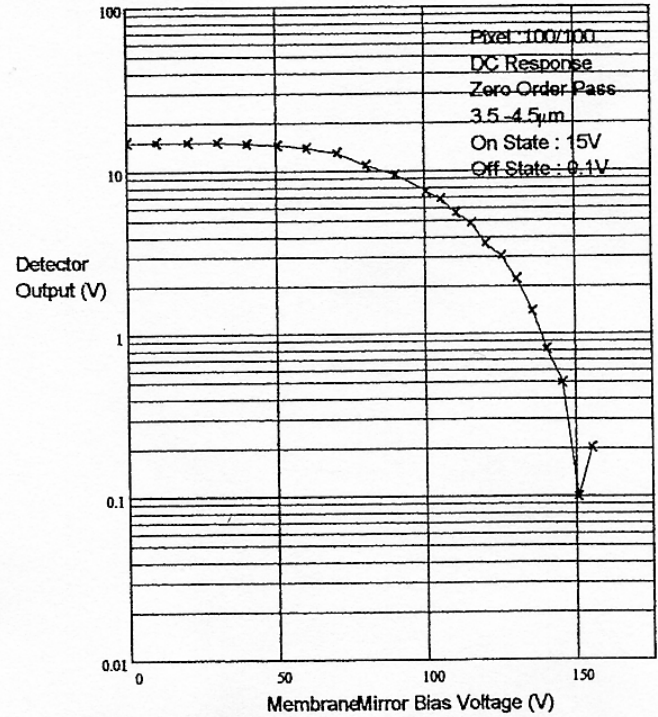


Figure 5: Measured static broadband-infrared zero-order-pass intensity characteristic of an MMLS with a 2-D array of pixels on a 100 μm pitch. The light has a central wavelength of 4.0 μm and half-widths at 3.5 and 4.5 μm.

3.3 Broadband Readout

To optimize the contrast ratio for zero-order-pass readout, there must be no overlap between the zero-order and the first-order spots in the Fourier plane so that a simple Fourier-plane aperture can be used to pass only the zero-order light. The shutter can be designed so that this condition is easily met for broadband light. When the shutter is operated with broadband light spanning a region between λ_{min} and λ_{max} , to optimize the contrast ratio the diameter W of the Fourier-plane spatial filtering stop (or aperture) should be chosen so that it is large enough to block (or pass) all the zero-order light, but small enough so as not to block (or pass) the first-order light. That is,

$$\frac{\lambda_{max} F}{D} < W < 2 \frac{\lambda_{min} F}{c} - \frac{\lambda_{min} F}{D}$$

where c is the pixel pitch, F is the focal length of the Fourier transform lens, and D is the effective diameter of the light beam. This constraint on separation of the orders becomes more difficult to meet as the collimation of the light is compromised more and more.

Figure 5 is a plot of the measured static broadband infrared intensity characteristic of an MMLS with a 2-D array of pixels on a 100-nm pitch in zero-order-pass operation. The central wavelength of the light is 4.0 μm and the half-width points are at 3.5 and 4.5 μm. Note that a contrast ratio of approximately 150:1 is achieved. Much higher contrast ratios are achieved by operating the device in the zero-order block mode. The infrared light was obtained by filtering a blackbody source with a long-pass 3.5-μm filter and a short-pass 4.5-μm filter.

3.4 Contrast Ratio

The contrast-ratio of the MMLS is frequency dependent. For zero-order-pass readout, the static contrast ratio is obtained by taking the ratio of the maximum output intensity (with no voltage across the device) to the

minimum output intensity (with V_{xi} across the wells). In this readout mode, the principal source of off-state radiance that can degrade the static contrast ratio is the non-ideal surface profile of the membrane mirror. The typical static zero-order pass contrast ratio for visible laser light has recently been improved to about 1,000:1, and 2000:1 is not unusual. Dynamic contrast ratio optimization in the zero-order-pass mode is achieved by setting the desired shutter frequency and adjusting both the dc voltage offset and the ac component of the driving signal voltage waveform to simultaneously minimize the off-state intensity and membrane ringing.

3.5. Shutter Speed

One of the key performance characteristics of the MMLS is the very short membrane deflection response time. The shutter speed is limited by the resonant frequencies of the membrane. In particular, if m is the areal mass density of the membrane, the first resonant frequency can be predicted from the equation

$$\omega_0 = \sqrt{\frac{16T}{ma^2}}$$

Thus, devices with small pixels can be operated at higher frequencies than devices with large pixels, but at the expense of higher operating voltages. For 50- μm -diameter well devices, the resonant frequency is approximately 1 MHz, and for 100- μm -diameter wells it is about 330 kHz. Figure 6 is a plot of the resonant frequency of membrane mirrors with circular pixels as a function of pixel diameter.

Square wave response (shutter operation) up to 1 MHz with minimal ringing has been demonstrated with a shutter employing 10- μm -diameter pixels. However, for large-pixel, low frequency (kHz) devices, it is often possible to use dc offset voltage to increase the effective membrane tension, and thereby push the first resonance to a higher frequency. This allows higher frequency operation, but at the possible expense of extinction ratio.

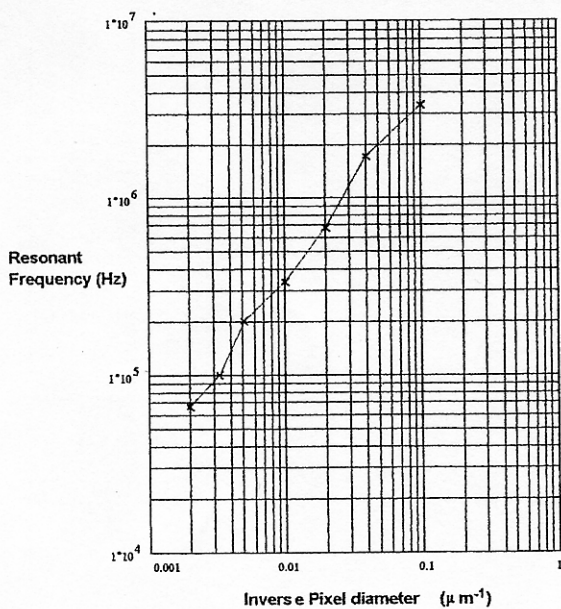


Figure 6: Resonant frequency of membrane mirrors as a function of pixel diameter

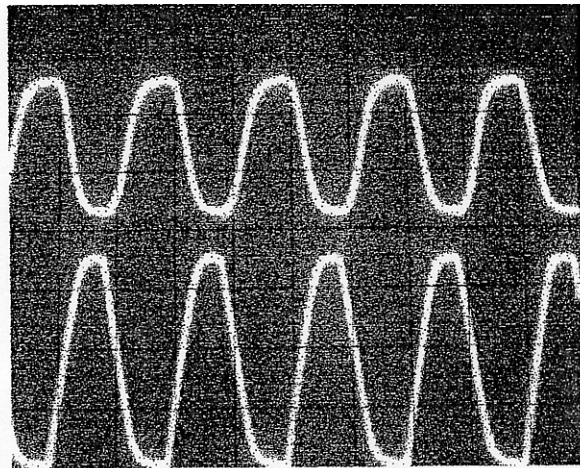


Figure 7: Zero-order intensity rise and fall characteristic (upper trace, 5V/div) of a 25- μm -diameter pixel device driven with a voltage waveform that swings between 0 and 170V (lower trace, 50V/div). The laser readout light has a wavelength of 633 nm. The time scale (horizontal) is 5 $\mu\text{s}/\text{div}$

Deformation/Recovery Time

The rise and fall times of the modulator are two of its most important characteristics. In the zero-order pass mode, the rise time is the membrane recovery time since the intensity in this readout mode increases as the

membrane recovers from its deformed state to the flat state. The membrane recovery time is dominated by the membrane tension. Similarly, for the zero-pass mode, the fall time is the membrane deformation time, and it is limited by the rise time of the driving amplifier. Figure 7 is an oscilloscope trace of the rise and fall zero-order intensity characteristic (upper trace) of a 25- μm -diameter pixel device driven with a voltage waveform that swings between 0 and 170V (lower trace). The laser readout light has a wavelength of 633 nm. The observed rise and fall times of the modulated light are at least 0.3 ns as they are almost identical to the rise and fall times of the driving signal. Devices with 50- μm diameter wells typically have rise times of about 7 p.s. One microsecond rise times are possible with 10- μm diameter pixels.

3.6. Non-periodic Pulse Operation and Waveform Shaping

The modulator performance is optimal for sinusoidal (sine-squared) drive signals, as smooth waveforms will minimize membrane ringing. For square wave and aperiodic pulse operation, especially for large-pixel ($> 100 \mu\text{m}$ diameter) devices, it is often advantageous to round the upper corners of the driving voltage waveform before applying it to the modulator. The intrinsic nonlinearity in intensity-voltage characteristic of the membrane mirror leads to an intensity pulse that is squarer than the rounded waveform driving pulse. Such a periodic train of rounded voltage pulses can be formed by adding some negative dc offset to a sine wave and applying this signal as input to a drive amplifier does not amplify the negative portion of the waveform. Adding additional de-offset to this waveform can further shape the intensity profile of the chopped light. DC-offset voltage increases the average tension of the membrane and thereby decreases the rise time of the shutter. However this is achieved at the expense of contrast ratio.

4. Selected Applications

By spatially filtering the MMLS output, controlled optical switching applications are enabled dependent upon the electrode structure that addresses the MMLS. Shuttered operation of the MMLS is configured by uniformly addressing the entire membrane by applying an electric field to all of the membrane wells within the device extent. By addressing the membrane mirror in this fashion, applications including large-area light beam modulation, white light (broadband) image shuttering (high-speed photography), laser pulse gating (LIDAR), high-power laser gating, optical encoding and printing, spectroscopy, are possible. We have used two shutter elements as seen in Figure 8 to create a broadband high-speed optical shutter. For this application, the device is designed with small wells (about 10^{th} pitch for operation at visible wavelengths) so that the zero-order image falls on the detector array and all the higher-order images fall outside the detector array. In this configuration using a white light source, we have measured 500:1 contrast ratio at switching speeds of 10 ns.

By addressing the MMLS with a pixelated electrode, we have created spatial light modulators capable of generating amplitude or phase images at wavelengths from the ultraviolet to the deep infrared spectrum. A variety of membrane-mirror light modulators have been made in the past using discrete addressing schemes [2-5]. More recently, we have built an MMLS on VLSI circuits producing a very compact spatial modulator package. A photograph of one of our membrane-over-VLSI devices is illustrated in Figure 9. In Figure 9a, we show the VLSI chip without the membrane attached and in Figure 9b, we show the VLSI chip with the membrane mirror applied. In this latter figure, one can observe the contact ring we employed in this experimental device to apply the electric field to the membrane mirror. On this high-voltage VLSI chip, we have completely integrated our addressing electronics for an 80×64 array onto a high-voltage VLSI substrate. This chip incorporates a 75×75 - μm pixel pitch and currently provides a 25V-drive range. A more complete analysis of this device and its optical performance will be the subject of a future publication.

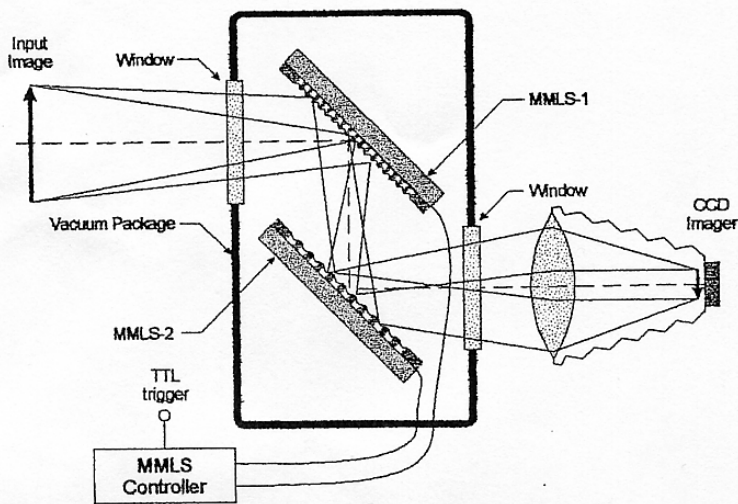


Figure 8: A setup illustrating the use of an MMLS for broadband image shuttering and gating.

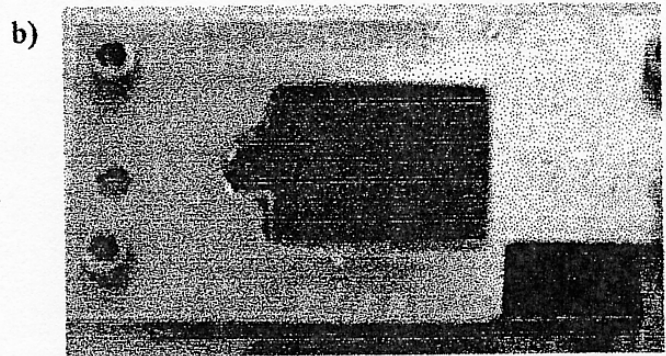
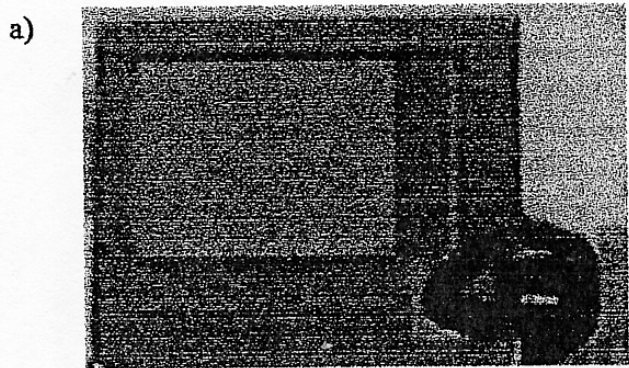


Figure 9: A high-voltage VLSI substrate: (a) without the membrane mirror applied and (b) the with membrane mirror applied.

5. References

1. K. Preston, Jr, "An Array Optical Spatial Phase Modulator," Proceedings of the IEEE International Solid State Circuits Conference, New York, 1968, p. 100
2. K. Preston, Jr., Coherent Optical Computers, (McGraw-Hill, New York, 1972), pp. 139-176.
3. L.E. Somers, "The Photoemitter Membrane Light Modulator Image Transducer," in Advances in Electronics and Electron Physics, Vol.33A (Academic Press, New York, 1972), 493.
4. K. Hess, R. Dandliker, and R. Thahnan, "Deformable Sill-face Spatial Light Modulator," Opt. Eng. 26, 418-422, 1987.
5. J.A. Van Raalte, "A New Schlieren Light Valve for Television Projection," Appl. Opt. 9, 2225-2230 (1970).
6. P. Reizman, "An Optical Spatial Phase Modulator Array Activated by Optical Signals," in Proceedings of the 1969 Electro-optical Systems Design Conference, pp225-230.
7. A.D. Fisher, L.C. Ling, J.N. Lee, and R.C. Fukuda, "Photoemitter Membrane light Modulator," Opt. Eng. 25, 261-268, 1986.
8. D.R. Pape, "Optically Addressed Membrane Spatial Light Modulator," Opt. Eng. 24, 107-110, 1985.
9. D.R. Pape and L.J. Hombeck, "Characteristics of the Deformable Mirror Device for Optical Information Processing, Opt. Eng. 22, 675-681, 1983.
10. L.J. Hombeck, "Defonnable-Muror Spatial Light Modulators," SPBE Critical Reviews 1150,86-102, 1989.
11. Horsky, T.N., C.M. Schiller, G.J. Genetti, D.M. O'Mara and C. Warde, "Electron-Beam-Addressed Membrane Mirror Light Modulator Projector Display System," Appl. Opt. 31, 3980-3990, 1992.
12. J. D. Gaskill, "Linear Systems. Fourier Transforms and Optics," Wiley, 1978.
13. L.C. Andrews, "Special Functions of Mathematics for Engineers," Oxford University Press, 2^o Edition, pp237.285.1998.
14. J.W. Goodman, "Introduction to Fourier Optics" McGraw Hill, 1968.